ISSN: 1813-4890

Research and Application of Similar Material Simulation Technology for Gob-side Entry Retaining with Gangue Filling

Shudong He

[1]State Key Laboratory of Coal Mine Disaster Prevention and Control, Chongqing 400037, China;

[2] China Coal Technology and Engineering Group Chongqing Research Institute, Chongqing 400037, China

Abstract

Aiming at the technology of gob-side entry retaining filled with gangue, this study employs similar material simulation methods and constructs a three-dimensional stereoscopic similar model to simulate the deformation, failure, and stress distribution patterns of overlying strata during the mining process. By comparing two support methods—a 2.5 m-thick gangue filling belt combined with single-row individual props and a 1.5 m-thick gangue filling belt combined with double-row individual props—it is found that as the mining face advances, the self-weight stress of the overlying strata increases, leading to multiple roof weightings and caving events. Among them, the 2.5 m gangue belt combined with single-row props exhibits poor support performance during roof weighting, with severe rock beam fractures and extensive roof caving. Conversely, the 1.5 m gangue belt combined with double-row props demonstrates better stability and support effectiveness, with rock layers bending and subsiding but experiencing less damage. The research results indicate that optimizing the width of the gangue filling belt and the arrangement of props can effectively enhance the stability of gob-side entry retaining, providing scientific evidence and technical support for coal mine safety production.

Keywords

Gob-side entry retaining; gangue filling; similar materials; simulation technology; stability.

1. Introduction

In the realm of coal mining, gob-side entry retaining (GER), as a vital branch of pillarless mining methods, demonstrates remarkable advantages [1-2]. Practical experience has shown that pillarless mining schemes can effectively control the occurrence of accidents such as gas explosions and rock bursts, providing strong guarantees for safe coal mine production. During the process of gob-side entry retaining, ensuring the stability of the roadway is a crucial aspect, which relies heavily on the support of roadside support systems[3]. However, gob-side entry retaining is subjected to intense mining-induced stresses during the pre-mining, post-mining, and subsequent working face mining stages. Particularly after the working face is extracted, severe subsidence of the roadway roof occurs, leading to a substantial increase in roadway deformation and failure range, posing significant challenges to roadway stability[4-6].

Given the importance and complexity of gob-side entry retaining technology, scholars both domestically and internationally have conducted extensive and in-depth research on this topic. The research primarily focuses on three areas: the study of surrounding rock movement patterns and the interaction between support and surrounding rock in gob-side entry retaining; roadside support technology; and roadway internal support technology, which encompasses

ISSN: 1813-4890

both primary and reinforcement support, with a variety of primary support forms including I-beam supports, U-shaped steel yieldable supports, bolt-cable support, and combined support systems[7-13]. Among the roadside support methods for gob-side entry retaining, gangue belt support has emerged as the preferred option due to its economic and environmental benefits. Transporting gangue underground for filling or support not only addresses environmental pollution and land occupation issues caused by large-scale gangue accumulation but also aligns with the requirements of sustainable development. When studying gob-side entry retaining technology supported by gangue belts, similar material simulation technology is a commonly employed approach.

Currently, research on similar material simulation experiment methods is advancing in two directions: planar strain models and three-dimensional (3D) solid models. Many leading rock mechanics research institutions are dedicated to developing relevant experimental apparatuses to facilitate 3D simulation studies of mining-induced stresses in coal mines [14-16]. By creating scaled-down models based on the actual prototypes of the simulated objects and conducting mining operations according to similarity ratios, the deformation, failure, and stress conditions of the models can be observed. This allows for the analysis and inference of actual on-site conditions, with simulation results exhibiting high reliability. Therefore, conducting research and application on similar material simulation technology for high-grade conventional mechanized gangue-filled gob-side entry retaining can provide reliable foundational data and practical references for safe coal mine production, holding significant practical importance.

2. Engineering Overview and Similarity Design

2.1. Overview

The East Wall 4 Working Face of the No. 3 Seam at the +570 m level in Muchengjian Coal Mine of Haohua Company is located within the No. 6 Crossheading at the +570 m level. The overlying No. 5 Seam has not been mined, while the underlying No. 2 Seam remains undisturbed. The western part of the working face has been arranged, the southern East Wall 3 has been extracted, the eastern part is adjacent to the goaf of Wall 4, and the northern part is currently under arrangement. This coal seam is a thin seam with a relatively complex structure, typically containing a layer of interbedded siltstone with a thickness ranging from 0.3 to 1.2 m. Based on a comprehensive analysis of the mining conditions surrounding the working face, the average thickness of the coal seam is determined to be 1.8 m, with an average strike direction of 70° and an average dip angle of 15°. The vertical distance to the No. 5 Seam ranges from 15 to 40 m, averaging 30 m, with the No. 5 Seam remaining unmined; the vertical distance to the No. 2 Seam ranges from 20 to 25 m, averaging 23 m, with the No. 2 Seam undisturbed. The geological structure of this working face is relatively complex. Based on the analysis of mining conditions at the working face, four faults are identified. Due to the influence of these faults, the roof and floor of the coal seam are fractured, necessitating enhanced management of the roof and floor during mining operations.

The basic conditions for simulation are as follows: (1) The average thickness of the No. 3 coal seam is 1.8 m, with an apparent density of 1.78 g/cm^3 and a uniaxial compressive strength of 7.79 MPa. (2) The immediate roof of the No. 3 coal seam consists of siltstone, with a thickness of 4 m. The measured uniaxial compressive strength of the rock stratum is 140.04 MPa, and the apparent density is 2.79 g/cm^3. (3) The immediate floor of the No. 3 coal seam has a thickness of 3 m. The measured uniaxial compressive strength of the rock stratum is 60.53 MPa, and the apparent density is 2.74 g/cm^3. (4) The inclined length (i.e., the length of the mining working face) of the No. 3 coal seam is 98 m, with an average inclination angle of 15°. (5) The measured uniaxial compressive strength of the gangue used for filling in the gob-side entry retaining of

ISSN: 1813-4890

the No. 3 coal seam is 48.73 MPa, with an apparent density of 2.67 g/cm^3. (6) Selection of gangue filling: Based on actual conditions, a three-dimensional model with reserved roadways will be adopted for comparative experiments. These experiments will involve a 2.5 m thick gangue filling belt combined with single-row individual props and a 1.5 m thick gangue filling belt combined with double-row individual props. The spacing between the double-row individual props is set at 2.5 m.

2.2. Similarity Model Design

The similarity principle dictates that the designed similarity model must adhere to the similarity relationships between the model and the prototype. To investigate the deformation, displacement, and caving patterns of the overlying roof rock following mining at the working face, it is imperative that the conditions occurring within the model faithfully replicate those in the prototype, thereby establishing the similarity relationships and criteria between the two. This model primarily focuses on the gangue filling technique for gob-side entry retaining in a single coal seam, featuring two reserved roadways. The coal seam has a thickness of 1.8 m. In the experiment, prefabricated gangue strips and single hydraulic cylinder supports will be placed within these roadways. The roof management will employ the natural caving method to study the patterns of mine pressure manifestation and the effectiveness of filling support during the natural caving of overlying strata as the working face advances. Therefore, a three-dimensional model frame measuring 1.9 m in length, 1 m in width, and 1.5 m in height will be utilized. The selected model has a length ratio and length similarity coefficient of 50, meaning that when the prototype length is 1 m, the corresponding length on the model is 2 cm. The prototype design for the similarity model is depicted in Figure 1 (units: m; scale: 1:500). Figure 2 illustrates the cross-section of gangue filling and support.

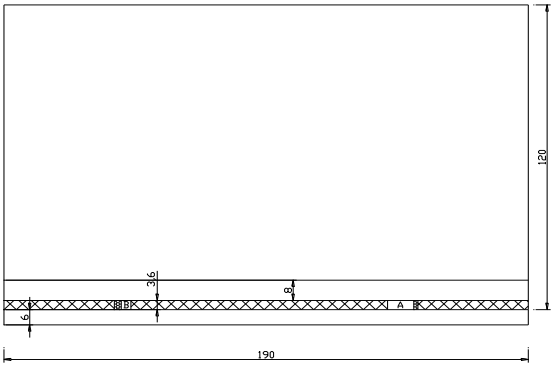

Figure 1 Prototype Design Diagram

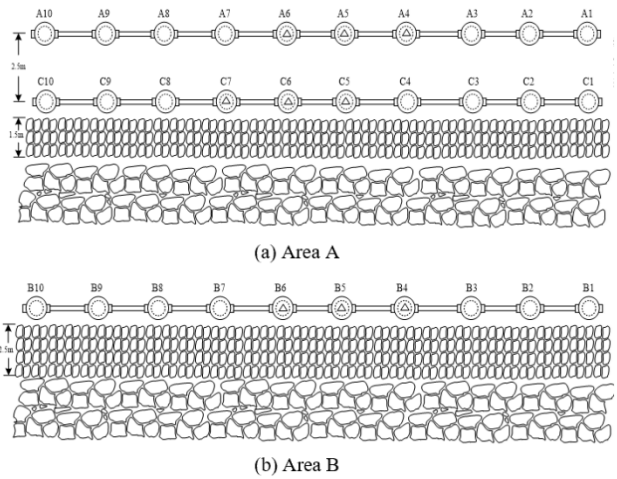

Figure 2 Sectional view of gangue filling and support

ISSN: 1813-4890

The No. 3 coal seam has a thickness of 1.8 m, with a siltstone floor measuring 3 m in thickness. The immediate roof of the No.3 coal seam consists of 4 m of siltstone, while the main roof is 12 m thick. In Zone B, a 2.5 m thick gangue filling belt combined with single-row individual props will be employed, whereas in Zone A, a comparative experiment will be conducted using a 1.5 m thick gangue filling belt combined with double-row individual props. The spacing between the double-row individual props is set at 2.5 m.

3. Design of Similar Material Proportioning and Filling

3.1. Design of Similar Material Proportioning

During the simulation of rock mechanics processes, it is essential to ensure that the compressive strength, tensile strength, flexural strength, elastic modulus, viscosity coefficient, plasticity, and rheological properties of the similar materials closely resemble those of the actual materials, while the Poisson's ratio and internal friction angle remain identical. Similar materials are typically formulated by blending several components, which can be categorized into skeletal materials and cementing materials based on their properties and functions. Generally, it is appropriate for the apparent density of similar materials to fall within the range of 1.5-1.8 g/cm^3. Excessive apparent density makes compaction difficult, while insufficient density results in loose and unstable model materials. The formation of similar materials must be completed before the initial setting of the cementing agent. Given that the initial setting time of gypsum, a common component in similar materials, is 7-8 minutes, a retarder must be added to extend the initial setting time to a suitable range of 15-20 minutes.

Standard test specimens are prepared using cylindrical molds with a height of 10 cm and a diameter of 5 cm, with four specimens forming a set. Based on different proportioning of similar materials and selected apparent densities ranging from 1.5 g/cm^3 to 1.8 g/cm^3, the total mass of the four standard specimens is calculated. The mass of water to be added is determined as one-tenth of the total mass of the mixed materials. Subsequently, the mass of a single standard specimen is calculated, and the material is poured into the mold. It is then compacted in layers using a tamping hammer until the desired height of the standard specimen is achieved. After curing for a specified period under natural indoor conditions, the mechanical properties of the standard specimens are immediately tested. The specific mechanical indicators to be measured are determined based on the research objectives under simulated conditions, and the testing must be conducted in accordance with the experimental procedures for the physical and mechanical properties of coal and rock. Prior to model fabrication, extensive work on similar material proportioning must be carried out. The uniaxial compressive strength values calculated based on stress similarity for the model should closely match or equal those measured from the similar material proportioning. If the discrepancy between the two exceeds 10%, the similar material proportioning must be redone until the tested strength equals or closely approximates (with a difference of less than 10%) the uniaxial compressive strength value on the model. The proportioning of similar materials is shown in the Table 1.

Table 1 Determination of similar material proportions

Rock name	Similar material ratio	Apparent density (g/cm3)	Water material ratio	Curing time (day)	Model calculation strength(MPa)	Similar proportioning strength(MPa)
Three slot coal seam	4:0.7:0.3 (Quartz sand: Lime: Gypsum)	1.5	1/9	3	0.131	0.134
Direct roof of	8:0.5:0.5 (Quartz sand:	1.7	1/10	7	1.707	1.760

ISSN: 1813-4890

three slot coal seam	Cement: Gypsum)					
Floor of three slot coal seam	9:0.5:0.5 (Quartz sand: Cement: Gypsum)	1.7	1/10	7	0.751	0.610
Gangue	9:0.5:0.5 (Quartz sand: Cement: Gypsum)	1.7	1/10	7	0.621	0.610

3.2. Filling and Observation Layout of the Similarity Model

This model frame employs a three-dimensional similarity material simulation test bench with a length of 1.9 m, a height of 1.5 m, and a width of 1 m. The formwork utilizes 12 cm channel steel. When laying the coal seam, the filling should be carried out in layers, with a minimum thickness of 1 cm and a maximum thickness of 2 to 2.5 cm. After the coal seam is filled, rock-similar materials are filled on top until reaching the top boundary of the model frame. Prior to model filling, the total mass of materials for a 2 cm-thick coal seam layer must be calculated. Specifically, when the vertical height of the rock stratum is 2 cm, calculate the volume of the quadrilateral layer, then multiply it by the apparent density of the model material to obtain the total mass per quadrilateral layer on the model. Based on the calculated total mass per layer, the quantity of each material required for each layer is determined. The preparation of the gangue belt differs slightly from the aforementioned method. First, calculate the mass of similar materials needed for gangue belts of different widths in Zones A and B. After proportioning the similar materials, package them in small bags using plastic wrap to simulate on-site gangue packaging in snakeskin bags. Subsequently, arrange three to four packaged gangue bags in a row and place them into pre-sealed transparent cloth bags with widths of 2.5 cm and 1.5 cm, respectively. After filling, the gangue bags are left to cure and set, as shown in Figure 3(a).

Nine pressure measurement points are set up in the two reserved roadway areas of the No. 3 coal seam, specifically located at the midpoints of the three rows of hydraulic cylinders in both Zones A and B, with three measurement points on each row of cylinders. Measurements are taken using high-precision CWY100 precision digital pressure gauges. The pre-prepared gangue belts are placed along the edges of the left and right reserved caving zones into the designated spaces. The two connected rows of hydraulic cylinders are then slowly positioned into the reserved spaces along the gangue belts in Zones A and B, as illustrated in Figure 3(b). All precision digital pressure gauges used for testing are connected to a computer via data cables, with each gauge linked to a single computer. The specialized software which means "supporting" or "accompanying" and can be translated as "accompanying" or omitted if the context makes it clear that the software is designed for the pressure gauges for these precision digital pressure gauges is employed to record the data, with a default recording interval of 2 seconds, meaning each gauge records 30 steady-state data points per minute. During the comparison of advancing the same distance in the mining face of the No. 3 coal seam, the roof pressure changes in the working face with gangue backfilling in the roadway are monitored using precision digital pressure gauges. Meanwhile, observations and records are made of the initial caving interval of the immediate roof and the periodic weighting interval at different mining distances in the mining face. The deformation, displacement, and caving conditions of the roof are observed. A steel ruler is employed to measure the deformation of the rock strata, the height of caving, and the caving angle of the rock strata, while a digital camera is used for documentation purposes.

ISSN: 1813-4890

(a) (b)

Figure 3 Filled Gangue Belts and Gangue Backfilling and Single Prop Support in Zone A

4. Observation Results and Analysis

4.1. Analysis of Observation Results from Measurement Points

High-precision digital pressure gauges were employed for direct testing, with data recorded every 2 seconds. From the pre-pressurization on the 16th to the post-mining stabilization period until the 29th, spanning a total of 13 days, 5,054,400 data points were collected from 9 measurement points. By plotting the data, the daily variation patterns for each measurement point were obtained. The measurement point data were first organized by eliminating outliers caused by power outages or disconnections, and then sampling every other data point for the remaining data. After data processing, curve fitting was performed to derive the pressure variation patterns of the overlying rock on the single props under different advancing distances of the mining face, considering scenarios with a single row of +2.5m gangue belt support (data from Measurement Point B) and double rows of +1.5m gangue belt support (data from Measurement Points A and C). Some of the calculated results are shown in Figure 4.

From the variation curves of the data from the three rows of measurement points, it can be observed that the data from Measurement Points A and C exhibit relatively smooth changes, whereas Measurement Point B shows frequent fluctuations, particularly following the initial significant pressure increase, with large-scale pressure pulsations. This indicates that the pressure changes experienced by the support props and the gangue belt are intense, suggesting poor support effectiveness. The data from the three measurement points in Row B are generally higher than those from Measurement Points A and C, indicating that the roof pressure under the single row of props combined with a +2.5m gangue belt is excessively high, resulting in inadequate support capacity. As the mining face continuously advances forward, the space within the mining face expands, causing the self-weight of the overlying rock strata to transfer to the sides of the reserved roadway, generating significant support pressure. When the rock strata reach their failure limit, severe damage occurs at the support points in front of and behind the mining face.

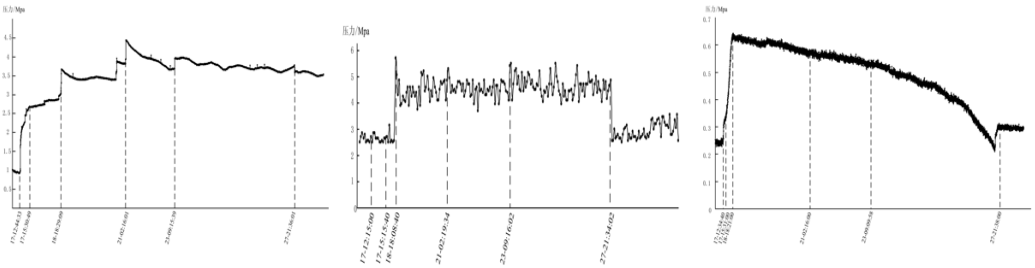

(a) A4 (b) B5 (c) C6

Figure 4 Curve of data changes at measurement points

4.2. Patterns of Roof Strata Behavior under Mining Pressure in the No. 3 Coal Seam

As the working face of the No. 3 coal seam continuously advances, the space within the mining face expands, causing the self-weight stress of the overlying rock strata to generate significant abutment pressure on the single props along the gob-side entry and the gangue belt, as well as

ISSN: 1813-4890

on the coal mass ahead of the working face. When the rock strata reach their failure limit, severe damage occurs at the support points in front of and behind the working face. As the roadways on both sides advance along with the working face, noticeable cracks are observed in the upper roof between the gangue belt and the single row of props in Zone B, tilting towards the caving zone, as shown in Figure 5(a). In contrast, under the same distance, no significant damage is evident in the upper roof between the gangue belt and the double rows of props in Zone A, as depicted in Figure 5(b).

When the mining face advances 34 m, distinct cracks appear in the coal mass ahead of the single row of props, running through the entire coal seam. This longitudinal crack is located 42 m from the single prop in front of the gangue belt, as illustrated in Figure 5(c). At this point, no significant cracks are found in the coal mass ahead of the double rows of props. When the left mining face advances to the 42 m mark where the longitudinal crack is located, the immediate roof experiences its first weighting, with an initial weighting interval of 42 m. The roof caving height is 2 m, and the roof separation is 1.5 m. The caved rock beam fractures in the middle, with a major fracture running through the entire caved roof and extending 42 m from the single props. The upper part of the rock beam rests on the single props behind the working face, while the lower part contacts the floor, with a lap length of 23.5 m. The middle section of the fractured rock beam touches the floor. At this time, the readings at various measurement points in Row B increase sharply, indicating significant roof pressure, as shown in Figure 5(d).

After the entire mining face is fully excavated, the immediate roof experiences its second weighting, causing the entire roof to cave. The upper rock beam of the immediate roof fractures into four segments, with the caved rock beams resting on the gangue belts and single props on both sides and contacting the floor at the bottom. At this point, the pressure readings at the measurement points for the single row of props fluctuate significantly, while the pressure values for the double rows of props increase noticeably. The roof pressure at this stage makes it difficult for the single props to bear the load, resulting in increased roof displacement in the working face of the No. 3 coal seam. The height of the 2.5 m gangue belt is compressed, while no significant changes are observed in the 1.5 m gangue belt, as shown in Figure 5(e). During the model stabilization period, the immediate roof experiences its third weighting, causing large-scale caving of the rock strata above the gob area in the No. 3 coal seam working face, with a caving height of 6.5 m. Only minor fissures exist between the rock strata, with minimal interlayer gaps. At this time, the pressure readings at the measurement points for the 2.5 m gangue belt combined with the single row of props in the left part of the No. 3 coal seam fluctuate frequently, with an increasing trend in amplitude and frequency. The left end of the rock beam fractures along the position of the single props, while cracks between the single props and the gangue belt extend upwards. The fractured rock beam leans towards the gangue belt, with more fractures on the left side. The caved rock beam has five distinct cracks running through the entire beam in the middle-left position, indicating the intense scope and magnitude of roof caving above the gob area, with significant impact intensity. The support effectiveness of the 2.5 m gangue belt combined with the single row of props is poor. The right end of the rock beam remains in contact with the double rows of props, with the entire beam bending and tilting towards the caving zone. No significant cracks are observed between the double rows of props and the gangue belt. The support effectiveness of the 1.5 m gangue belt combined with the double rows of props is satisfactory, as shown in Figure 5(f).

ISSN: 1813-4890

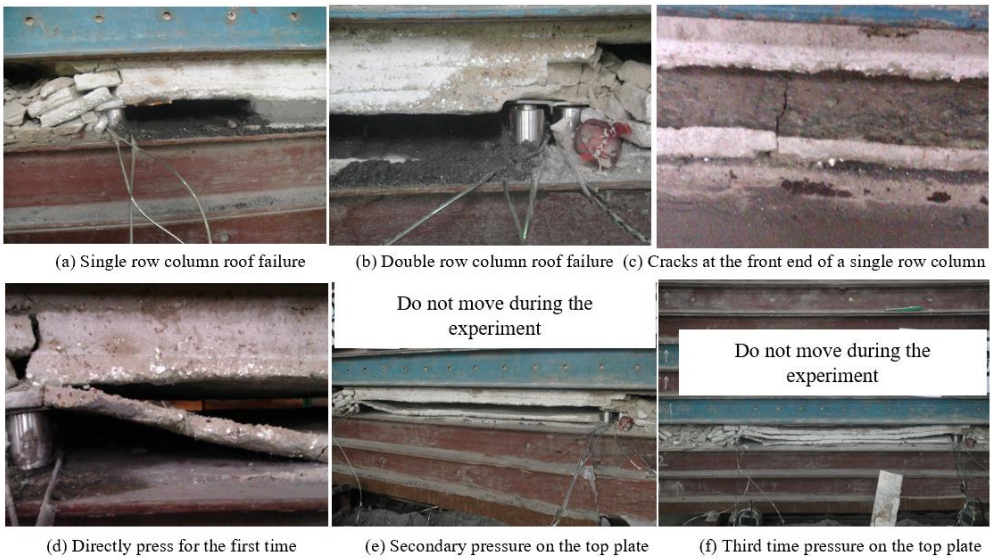

(a) Single row column roof failure (b) Double row column roof failure (c) Cracks at the front end of a single row column

(d) Directly press for the first time (e) Secondary pressure on the top plate (f) Third time pressure on the top plate

Figure 5 Experimental observation chart

During the continued standing period, the immediate roof underwent its fourth weighting. The maximum caving height of the immediate roof reached 17.5 m, with a maximum roof separation of 2.3 m. The caved rock beam rested on the supporting ends on both sides of the gangue-filled gob-side entry, spanning a length of 94 m, and contacting the floor over a length of 76 m. A prominent crack was observed in the middle of the caved rock beam, located 46 m from Zone B. Due to the self-weight stress of the overlying rock beams, two caving lines appeared in the overlying strata at the end of the working face. The presence of these two caving lines in the upper strata poses risks to the safety of mining operations in the No. 3 coal seam working face and also affects the success of the gob-side entry retention. The caving angle of the rock strata at the left end of the gob area was 68°, while at the right end, it was 66°. Upon observing the support conditions in Zones A and B during the final caving scenario, it was found that the failure mode in the area with a 2.5 m gangue belt combined with a single row of props was primarily characterized by multiple cracks in large rock beams. The support zone suffered severe damage, with the roof rock beams fracturing into multiple pieces and tilting towards the original caving area. The intense abutment pressure and the downward sliding force of the rock strata caused severe bending and failure of the immediate roof rock beams at the lower end. Additionally, noticeable cracks were present both behind the gangue belt and between the gangue belt and the single props, with the cracks between the supports being particularly prominent, as shown in Figure 6(a). In contrast, the failure mode in the area with a 1.5 m gangue belt combined with double rows of single props was more regular. The bending and subsidence of the rock strata resulted in large-scale roof caving across the entire length of the working face. However, the failure cracks were relatively small and fully compacted, with no significant cracks observed in the upper part of the support zone or in the areas ahead and behind it, indicating a satisfactory support effect, as shown in Figure 6(b).

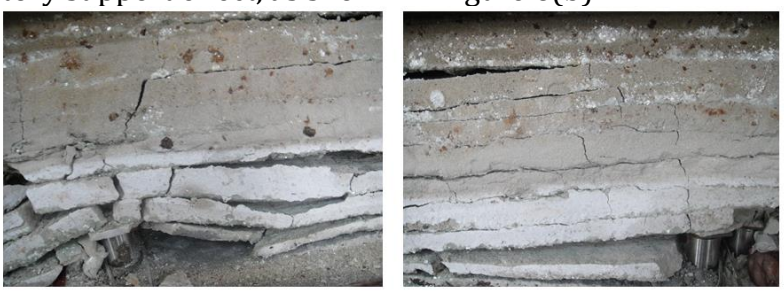

(a) Single row column (b) Double row column

Figure 6 Final top plate failure diagram

ISSN: 1813-4890

5. Conclusion

(1) As the working face of the No. 3 coal seam continuously advances, the space within the mining face expands. The self-weight of the overlying rock strata above the working face is transferred to both sides of the mining face space, creating significant abutment pressure. This exerts strong support pressure on the single props along the gob-side entry, the gangue belt, and the coal mass ahead of the working face.

(2) When the entire mining face is fully excavated, the immediate roof experiences its second weighting, leading to the collapse of the entire roof. The upper rock beam of the immediate roof fractures into four segments, with the caved rock beams resting on the gangue belts and single props on both sides and making contact with the bottom. At this point, the roof pressure makes it difficult for the single props to bear the load, and both the gangue belt and the single row of props are subjected to severe pressure. The roof displacement in the working face of the No. 3 coal seam increases. The height of the 2.5 m gangue belt is compressed, while no significant changes are observed in the 1.5 m gangue belt.

(3) During the model standing period, when the immediate roof undergoes weighting, large-scale caving occurs in the rock strata roof above the gob area of the No. 3 coal seam working face. The left end of the rock beam fractures along the position of the single props, while cracks between the single props and the gangue belt extend upwards. The fractured rock beam leans towards the gangue belt, with more fractures occurring on the left side. The caved rock beam has five distinct cracks running through the entire beam in the middle-left position. The support effectiveness of the 2.5 m gangue belt combined with a single row of single props is poor. The right end of the rock beam remains in contact with the double rows of props, with the entire beam bending and tilting towards the caving zone. No significant cracks are observed between the double rows of single props and the gangue belt. The support effectiveness of the 1.5 m gangue belt combined with double rows of single props is satisfactory.

Acknowledgments

The study was supported by the State Key Laboratory at China Coal Technology and Engineering Group Chongqing Research Institute (2025YBXM36).

References

[1] Sun Henghu. New Research on the Roof Activity Mechanism and the Relationship Between Support and Surrounding Rock in Gob-Side Entry Retaining [D]. Beijing: China University of Mining and Technology Beijing Graduate School, 1988.

[2] Sun Henghu, Zhao Bingli. Theory and Practice of Gob-Side Entry Retaining [M]. Beijing: Coal Industry Press, 1993.

[3] Jia Housheng, Wang Yibo. Load-Bearing Characteristics of Crushed Stone Pillars in Goaf and Stability Mechanism of Gob-Side Entry Retaining in Steeply Inclined Coal Seams [J]. Journal of China University of Mining & Technology, 2025, 54(03): 561-576.

[4] Qi Taiyue. Theoretical Research and Case Analysis of Support in Gob-Side Entry Retaining [D]. Xuzhou: China University of Mining and Technology, 1996.

[5] Qi Taiyue, Guo Yuguang, Hou Chaojiong. Study on the Adaptability of Integral Casting Roadway Protection Zone in Gob-Side Entry Retaining [J]. Journal of China Coal Society, 1999(3).

[6] Xin Yajun, Tian Menghan. Synergistic Load-Bearing Mechanism Between Gob-Side Support Body and Accumulated Body in Gob-Side Entry Retaining [J]. Journal of China University of Mining & Technology, 2025, 54(03): 595-608.

[7] Shi Xianying, Tian Zhicheng. Study on the Deformation Mechanism of Surrounding Rock in Gob-Side Entry Retaining Under Secondary High-Intensity Mining [J]. China Mining Magazine, 2025, 34(05): 187-197.

ISSN: 1813-4890

[8] Xie Wenbing. Stability Analysis of Surrounding Rock in Gob-Side Entry Retaining with Fully Mechanized Top-Coal Caving [J]. Chinese Journal of Rock Mechanics and Engineering, 2004, 23(18): 3059–3065.

[9] Gao Jinbo, Jing Yongjia. Mechanism of Lateral Load Action on Gob-Side Support and Load Reduction Control Technology in Gob-Side Entry Retaining [J]. Coal Engineering, 2025, 57(03): 115-125.

[10] Liu Zilu, Yu Weijian, Ma Zhanguo, et al. Load-Bearing Law and Instability Criterion of Pier Support on Gob Side in Gob-Side Entry Retaining of Fully Mechanized Caving Face [J]. Journal of China Coal Society, 2025, 50(05): 2394-2412.

[11] Chu Xinyu, Cui Haifeng, Li Zhen'an, et al. Roof Structure Control and Rational Gob-Side Support in Gob-Side Entry Retaining Under Close-Range Coal Seam Goaf [J]. China Coal, 2025, 51(02): 45-58.

[12] Wang Jun, Yan Chaochao. Influence of Section Coal Pillar Recovery on Surrounding Rock Instability and Control Technology in Gob-Side Entry Retaining [J]. Coal Engineering, 2024, 56(11): 38-45.

[13] Yang Gengqun, Wang Jun, Sun Yongkang, et al. Study on Gangue Concrete Backfill Material and Reasonable Width for Gob-Side Support [J]. Safety in Coal Mines, 2024, 55(11): 166-175.

[14] Liu Chunlin. Study on the Reasonable Width of Gob-Side Backfill Body in Semi-Coal Rock Roadway [J]. Journal of Shanxi Institute of Energy, 2022, 35(06): 22-24.

[15] Li Peng, Zhu Yongjian, Wang Ping, et al. Reasonable Width and Yielding Scale of Gob-Side Support Body in Steeply Inclined Thick Hard Roof [J]. Journal of Central South University (Natural Science Edition), 2022, 53(11): 4494-4503.

[16] Gong Peng, Ma Zhanguo, He Zexin, et al. Evolution Mechanism of Surrounding Rock Structure in Gob-Side Entry Retaining with Gangue Backfilling [J]. Journal of Mining & Safety Engineering, 2023, 40(04): 764-773+785.